Diffusion on a DLA cluster in two and three dimensions

1994 J. Phys. A: Math. Gen. 27 4341

(http://iopscience.iop.org/0305-4470/27/13/010)

J. Phys. A: Math. Gen. 27 (1994) 4341–4350. Printed in the UK

Diffusion on a DLA cluster in two and three dimensions

Donald J Jacobs†‡, Sonali Mukherjee† and Hisao Nakanishi†

† Department of Physics, Purdue University, West Lafayette 47907, USA

‡ Institute for Theoretical Physics, State University, Princetonplein 5, PO Box 80006, 3508 TA Utrecht, The Netherlands

Received 20 April 1994

Abstract. We present a much improved calculation of the dynamic critical exponents of diffusion d_w, d_s, and the combination d_f/d_w for the DLA (diffusion-limited aggregate) on square and simple cubic lattices using two independent approaches, one based on the exact enumeration for the displacement and velocity autocorrelation and the other on the eigenspectrum of random walks on the DLA. The two methods give consistent results, which, however, clearly rule out the scaling relation $d_s = 2d_f/d_w$ first proposed by Alexander and Orbach, similarly to the case of the Eden tree reported previously.

1. Introduction

Some time ago Dhar and Ramaswamy [1] considered diffusion on a simple tree-like structure which they called the Eden tree, and concluded that a typical random walk samples only order-1 segments (or a *branch*) of the backbone so that the commonly accepted scaling relation due to Alexander and Orbach [2],

$$d_s = 2d_f/d_w \tag{1}$$

does not hold (for the Eden tree, $d_f = d$ since they are compact). Their work was later confirmed by a different method and further extended to three dimensions by Nakanishi and Herrmann [3].

Diffusion on tree-like (or loopless) structures can present qualitatively different behaviour compared to that on a structure with many loops (especially large scale loops) because of the possibility of trapping in the loopless case. The scaling derivation of (1) requires that the fractal dimension of the region visited by the random walk be the same as that of the entire substrate, which may be violated if such trapping occurs.

Tree-like structures arise in many situations in statistical physics. A typical example is the DLA (diffusion-limited aggregate) [4] which is a very common model of various irreversible growth processes. The DLA is tree-like on large scales although not strictly loopless on small scales. Thus a DLA cluster provides an important structure for testing the extent to which the breakdown of (1) may be universal to tree-like structures. Considering random walks confined to move on a DLA cluster of fixed size, S, we have conducted a detailed study of the dynamical exponents of diffusion on the DLA. The exponents we calculate include the walk dimension, d_w, and the spectral dimension, d_s, which for an infinite cluster are defined by the asymptotic relations

$$\langle R(t)^2 \rangle \sim t^{2/d_w} \tag{2}$$

0305-4470/94/134341+10$19.50

where $\langle R(t)^2 \rangle$ is the mean-square displacement of a t-step random walk, and

$$P(t) \sim t^{-d_s/2} \tag{3}$$

where $P(t)$ is the mean probability that a random walk returns to its starting point at the tth step.

We emphasize that the dynamics of a random walk is considered only after a DLA cluster has been grown. The DLA is grown from a seed site by starting a single diffusing particle (modelled by a random walk) at a distance far from the centre of mass of the aggregate and waiting until the particle reaches one nearest neighbour distance from any site within the aggregate. At this time the particle sticks with probability one and then a new particle is released until the cluster reaches the desired size S. The random walk of the particle is performed off lattice until it becomes sufficiently close to a site of the aggregate where upon the particle is restricted to move on the underlying lattice. Our algorithm closely follows the techniques described by Vicsek [5]. The fractal dimension of our aggregates in two and three dimensions was found to be $d_f = 1.70 \pm 0.02$ and 2.48 ± 0.02, respectively.

Previously, Meakin and Stanley [6] have calculated the exponents d_w and d_s from Monte Carlo simulations of random walks on DLA clusters. Combining with their own estimates for the exponent d_f, their results indicated that $2d_f/d_w = 1.35 \pm 0.1$ and 1.44 ± 0.2 in two and three dimensions, respectively, whereas their direct estimates of d_s were 1.20 ± 0.1 in $d = 2$ and 1.30 ± 0.1 in $d = 3$. If currently accepted estimates for the fractal dimension [5] were used, their results would indicate $2d_f/d_w = 1.31 \pm 0.1$ in $d = 2$ and 1.50 ± 0.1 in $d = 3$. Thus, there was a strong suggestion of the breakdown of (1) already, which was, however, obscured by large error bars. Actually, as is commonly done, Meakin and Stanley [6] used (1) as an alternative *definition* of d_s, and their work concentrated on the dimensional dependence of d_s.

Webman and Grest [7], on the other hand, calculated d_s by diagonalizing a Hamiltonian for a corresponding elasticity problem [2], and obtained the estimates $d_s = 1.10 \pm 0.05$ in two dimensions. They also gave an argument for an upper bound for d_s of $2d_f/(d_f + 1) = 1.309\ldots$ for two dimensions. Although they noted the discrepancy between their estimate of d_s and the estimate of $2d_f/d_w$ of [6], no inferences were made from this observation.

In this paper, we use two independent approaches to explicitly evaluate the dynamical exponents d_w, d_s, and the ratio d_f/d_w. The first approach uses an exact enumeration method to calculate the mean-square displacement $\langle R(t)^2 \rangle$ and the velocity autocorrelation $\langle v(t) \cdot v(0) \rangle$ of the random walk on the DLA, while the second calculates the eigenspectrum of the transition probability matrix associated with the random walk on the DLA. In both methods many independent realizations of the DLA clusters are considered which were generated using the same growth algorithm. Each of these approaches and the results are described in the following sections. We summarize the results in the final section.

2. Exact enumeration approach and results

As described elsewhere in more detail [8, 9], the discrete time–velocity autocorrelation function for a random walker confined to a cluster of S sites can be easily calculated by exact enumeration. For a given cluster, all possible Brownian paths are summed over, starting from all sites, s, (where $1 \leqslant s \leqslant S$) weighted by the stationary probability distribution, $\rho(s)$. The exact enumeration is performed by successive multiplications of the transition probability matrix **W**. The matrix, **W**, is a stochastic matrix with elements W_{s_2,s_1} that give

the hopping probability of the random walk from site s_1 to site s_2. In particular, we calculate the velocity autocorrelation function by

$$\langle v(t) \cdot v(0) \rangle = \sum_{\{s_j\}_{j=1}^{t+1}} [r(s_{t+1}) - r(s_t)] \cdot [r(s_1) - r(s_0)] \prod_{i=1}^{t+1} W_{s_i, s_{i-1}} \rho(s_0) \quad (4)$$

where $r(s)$ is the position vector of site s. The mean-square displacement of the random walker is obtained by two summations of the velocity autocorrelation function [8] over the discrete time t. We have used the myopic-ant rule where the walker always hops to one of its nearest neighbours with equal probability at each time-step.

We now extend the meaning of the average of a quantity, A, denoted by $\langle A \rangle$ to include a second average over an ensemble of clusters of size S. The number of realizations averaged over and the corresponding maximum time-steps for each selected size are summarized in table 1.

Table 1. Summary of exact enumeration parameters for each cluster size S. N denotes the number of realizations averaged over and t_{max} denotes the maximum time-step calculated.

S	N $(d=2)$	t_{max} $(d=2)$	N $(d=3)$	t_{max} $(d=3)$
625	400	10 000	600	10 000
1 250	200	70 000	300	20 000
2 500	100	100 000	200	50 000
5 000	60	100 000	120	100 000
10 000	30	100 000	70	100 000
20 000	108	100 000	30	100 000
40 000	10	100 000	16	100 000
80 000	30	10 000	36	10 000

We make a finite-size scaling assumption that the mean-square displacement for t, $s \to \infty$ has the functional form

$$\langle R(t, S)^2 \rangle = R_\infty(S)^2 F[t/\tau] \quad (5)$$

where $R_\infty(S)^2$ is the saturation value for clusters of size S, τ is the characteristic time that a typical random walk will explore the entire cluster, and the scaling function $F(x)$ must have the limits

$$\lim_{x \to \infty} F(x) \to 1 \qquad \lim_{x \to 0} F(x) \to x^{2/d_w} \quad (6)$$

so that the asymptotic dependence of an infinite cluster is recovered for $x = t/\tau \ll 1$. Since $R_\infty(S)$ for a given cluster is just the radius of gyration, using the scaling form of (2) up to $t \approx \tau$, we can write the characteristic time as

$$\tau(S; d_w) = R_\infty(S)^{d_w} \quad (7)$$

where we show an explicit dependence on the walk exponent to remind the reader that we do not know d_w in advance.

In figure 1, we plot $\langle R(t, S)^2 \rangle / R_\infty(S)^2$ against $x = t/\tau(S)$ on logarithmic scales for both two and three dimensions. Note that only d_w has been adjusted to make the data for

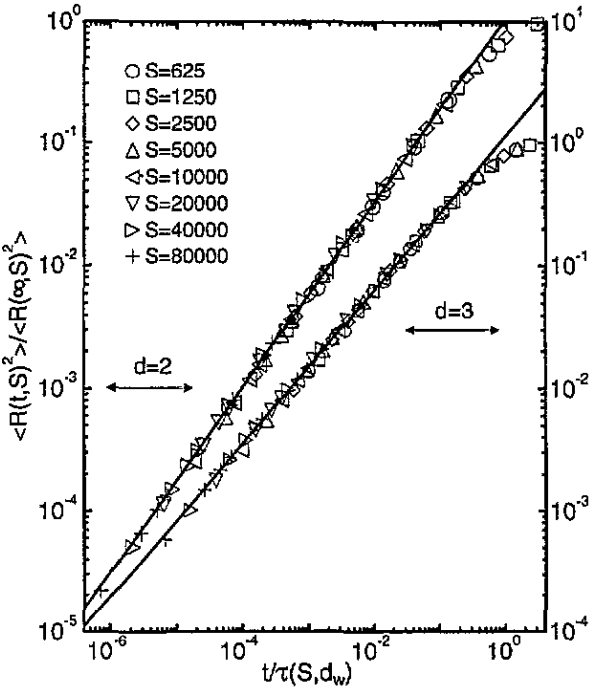

Figure 1. The mean-square displacement normalized by its saturation value for various sized clusters is plotted against the scaled time $x = t/\tau(S; d_w)$ on logarithmic scales. To keep the $d = 2$ and $d = 3$ curves separated, different abscissa scales are used to the left- and right-hand sides, respectively. The full lines correspond to the asymptotic scaling behaviour described by (2) with the numerical value for d_w chosen to be 2.64 for 2D and 3.19 for 3D. Only some of the data points are shown for larger t to avoid overcrowding.

different sizes collapse onto one curve. The estimation for d_w from best data collapsing is checked for self-consistency by least-square fitting of the data in the power-law regime ($x \ll 1$) where the slope should equal $2/d_w$. Since we expect (5) and (7) to only be valid for times long enough for the fractal nature of the cluster to be probed, we fit over a range $t \geqslant t_{min}$ where t_{min} has been varied between 10–1000. The measured slope is sensitive to the precise upper cut-off in x and the lower cut-off in t. The error bars quoted have been estimated by taking into account the sensitivity of the fitting range as well as the visual appearance of the data collapse onto a single curve. From the above procedure, we have determined $d_w = 2.64 \pm 0.05$ for two dimensions and 3.19 ± 0.08 for three dimensions. With our independent estimates for the fractal dimension d_f, we obtain $2d_f/d_w$. These results are summarized in tables 3 and 4.

We estimate the spectral dimension d_s by using the fact that the velocity autocorrelation function for the myopic ant on bipartite clusters exhibits a strongly oscillating behaviour [8]. The bipartite nature of the clusters is enforced by using a square or simple cubic lattice in generating the DLA. That is, all sites within the DLA cluster are subdivided into two distinct sets having a particular parity. A parity of $\chi(s) = +1$ is assigned to any site on one sublattice (i.e. for s where the sum of its coordinates is even) and -1 is assigned for the sites on the other sublattice. The strong oscillation is a consequence of the fact that a myopic ant must hop between the sites of opposite parity at each time-step.

We break the velocity autocorrelation function into a sum of two parts, each defined as

$$\phi_c(t, S) = \tfrac{1}{2}[\langle v(t) \cdot v(0)\rangle + \tfrac{1}{2}(\langle v(t+1) \cdot v(0)\rangle + \langle v(t-1) \cdot v(0)\rangle)] \tag{8}$$

and

$$\phi_0(t, S) = \langle v(t) \cdot v(0)\rangle - \phi_c(t, S) \tag{9}$$

where the S dependence on the right-hand side is implicitly understood. The contribution from the centre line, $\phi_c(t, S)$, is responsible for the observed anomalous diffusion and decays as a power law in t with the exponent $2/d_w - 2$. The envelope of the oscillating part of the velocity autocorrelation function, $\phi_0(t, S)$, has been found [8] to decay as a power law in t which can be related to the spectral dimension.

To make the connection to the spectral dimension, we first note that the envelope of oscillation does not decay to zero for any finite S, but rather to a non-zero residue, $|\phi_\infty(S)|$. This residual value can be calculated by

$$|\phi_\infty(S)| = \langle u \cdot u\rangle \qquad u = \sum_{s=1}^{S} r(s)\chi(s)\rho(s)\,. \tag{10}$$

As shown previously for percolation clusters [8], the scaling relation $|\phi_\infty(S)| \sim 1/S$ (for large S) also holds for the DLA.

Secondly, we extend the scaling of ϕ_0 to finite t by making the ansatz that the envelope will decay in t as the inverse of the number of distinct sites visited (denoted as $\langle N(t, S)\rangle$, where $\langle N(\infty, S)\rangle = S$). That is,

$$|\phi_0(t, S)| \sim 1/\langle N(t, S)\rangle\,. \tag{11}$$

Since the probability of returning to the starting point is also inversely proportional to $\langle N(t, S)\rangle$, it follows that $|\phi_0(t, \infty)| \sim t^{-d_s/2}$. Numerical support for this form of decay in the percolation problem was given in [10] from the eigenspectrum analysis near the negative maximum eigenvalue.

Finally, we make a finite-size scaling ansatz

$$|\phi_0(t, S)|^{-1} = S\, G\big(tS^{-2/d_s}\big) \tag{12}$$

where the scaling function $G(x) = N(t, S)/S$ will have the limiting behaviour

$$\lim_{x\to\infty} G(x) \to \text{constant} \qquad \lim_{x\to 0} G(x) \to x^{d_s/2} \tag{13}$$

recovering the asymptotic dependence $t^{-d_s/2}$ when $\langle N(t, S)\rangle/S \ll 1$.

In figure 2, we plot $G(x)$ against $x = t/S^{2/d_s}$ on logarithmic scales for both two and three dimensions. Only d_s is adjusted to make the data for different sized clusters collapse onto one curve. The procedure in estimating d_s is the same as discussed above for d_w. Note that we have developed the scaling of the data using the cluster size S. Alternatively, we can also scale with ϕ_∞. The latter procedure gave essentially the same results but with larger statistical fluctuations.

The scaling form of (12) appears to be obeyed rather well in figure 2 for $x \leqslant 1$. However, the data splits into multiple curves for $x \geqslant 1$, where saturation sets in earlier with the smaller clusters. This size-dependent trend may be caused by corrections to the $1/S$ scaling law, but the larger statistical fluctuations for larger S and t prevented us from studying the region $x \geqslant 1$ more carefully. Nevertheless, the excellent scaling for $x \leqslant 1$ has allowed us to determine $d_s = 1.20 \pm 0.05$ for two dimensions and 1.35 ± 0.05 for three dimensions.

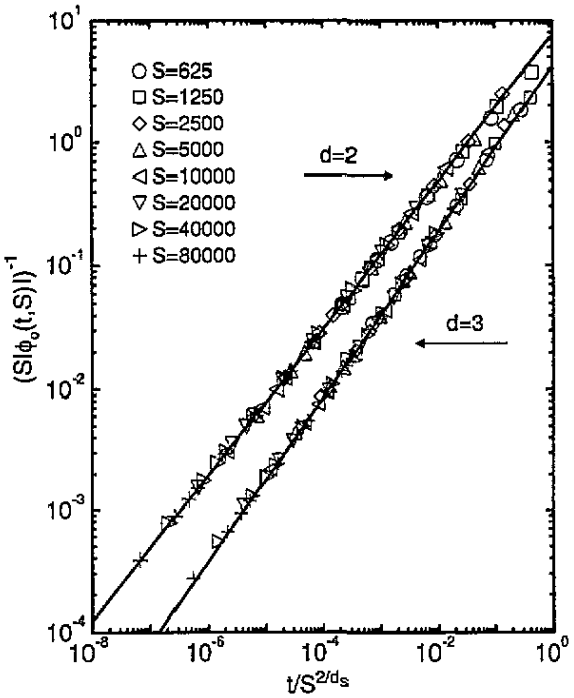

Figure 2. The inverse of the envelope of the oscillating part of the velocity autocorrelation function scaled by the the cluster size is plotted against the scaled time $x = t/S^{2/d_s}$ on logarithmic scales. The full lines correspond to the asymptotic scaling behaviour of $\sim t^{d_s/2}$ with the numerical value for d_s chosen to be 1.20 for 2D and 1.35 for 3D.

3. Eigenspectrum approach and results

In this section we briefly describe the spectral analysis of the transition probability matrix **W**. For simplicity we have used the blind-ant rule for the hopping probability of the random walk for the present approach. The estimated critical exponents are not sensitive to this choice of ant. The blind ant hops to an available nearest neighbour with probability $1/z$, and remains at the same site with probability $1 - m/z$, where z is the coordination number of the lattice and m is the number of available nearest neighbours.

The spectral dimension d_s is estimated from the density of eigenvalues, $n(\lambda)$, of **W**. In particular, for the eigenvalues λ near unity, we have [10, 11]

$$n(\lambda) \sim |\ln \lambda|^{d_s/2-1}. \tag{14}$$

The power-law scaling described by (14) occurs for $|\ln(\lambda)| \ll 1$ because $n(\lambda)$ is the inverse Laplace transform of the return to the starting point probability $P(t)$, which has the asymptotic form of (3). We take $n(\lambda)$ to be normalized such that $\sum_\lambda n(\lambda) = 1$, where in the case of the blind ant, λ is real and $-1 < \lambda \leqslant 1$.

A direct estimate of the ratio d_w/d_f can be made by applying finite-size scaling to the second largest eigenvalue, λ_2, where

$$|\ln \lambda_2| \sim S^{-d_w/d_f}. \tag{15}$$

Note that the largest eigenvalue is equal to unity corresponding to the stationary state. The scaling law of (15) follows from first noting that the decay timescale of each mode

is governed by $t \sim |\ln\lambda|^{-1}$. Secondly, the slowest decaying mode corresponding to the eigenvalue λ_2, is expected to have non-negligible eigenvector components that extend over the entire cluster. Therefore the slowest decay time, t_2, corresponds to the timescale that a random walk has probed the entire cluster, as defined in (6), implying $t_2 \sim S^{d_w/d_f}$. The finite-size scaling of λ_2 has been discussed previously in more detail and verified for percolation clusters [12].

The matrix **W** has been numerically diagonalized using the Arnoldi–Saad algorithm [13]. It allows us to extract a subset of eigenvalues of **W** which are close to unity by diagonalizing a subspace of **W** rather than the entire matrix, which makes the algorithm highly efficient. The merits of using this algorithm over other diagonalizing routines were given explicitly in [11]. We obtained the eigenvalues by this method which are accurate up to 10^{-6}. The precise number of eigenvalues that can be found accurately depends on various parameters such as the size of the subspace. The number of independent realizations used to obtain the average of the quantities $n(\lambda)$ and λ_2 are summarized in table 2.

Table 2. Summary of eigenspectrum analysis parameters for each cluster size S. N denotes the number of realizations averaged over.

S	N ($d = 2$)	N ($d = 3$)
100	4000	4000
400	3500	3000
1000	1000	1000
5000	2000	1050

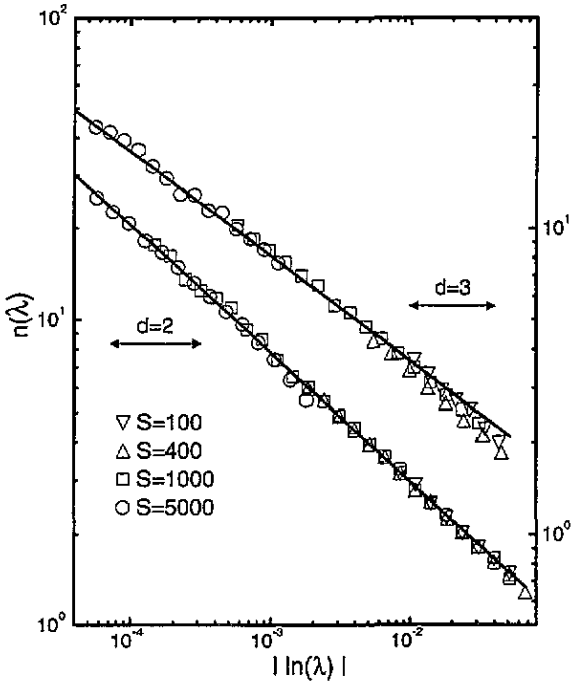

Figure 3. The normalized density of eigenvalues for various size clusters is plotted against $|\ln(\lambda)|$ on logarithmic scales. Different abscissa scales are used to separate the 2D and 3D data. The full lines correspond to the asymptotic scaling behaviour described by (14) with the numerical value for $1 - d_s/2$ chosen to be 0.42 for 2D and 0.345 for 3D. These power-law exponents were estimated by extrapolating to infinite cluster size, as explained in the text.

In figure 3 we plot $n(\lambda)$ against $|\ln\lambda|$ on logarithmic scales for both two and three dimensions. In two dimensions, the data from the various sized clusters collapse well onto a single curve; thus indicating that finite-size corrections are negligible. The slopes of the individual data sets do not vary appreciably from the collective data over all sizes from which $d_s/2-1$ is obtained. In three dimensions, the data collapse is not as good, which may be an indication of finite-size effects. A slight dependence on the cluster size of the individual slopes was found. By extrapolating the slopes (obtained from least-squares fitting) of the individual data sets for size S, against $1/S$, we have estimated $d_s/2-1$ applicable for an infinite cluster. In this way we have determined $d_s = 1.16 \pm 0.01$ in two dimensions and 1.31 ± 0.02 in three dimensions. The error bars quoted have taken into account the the variation in slopes and the extrapolation procedure for $d = 3$.

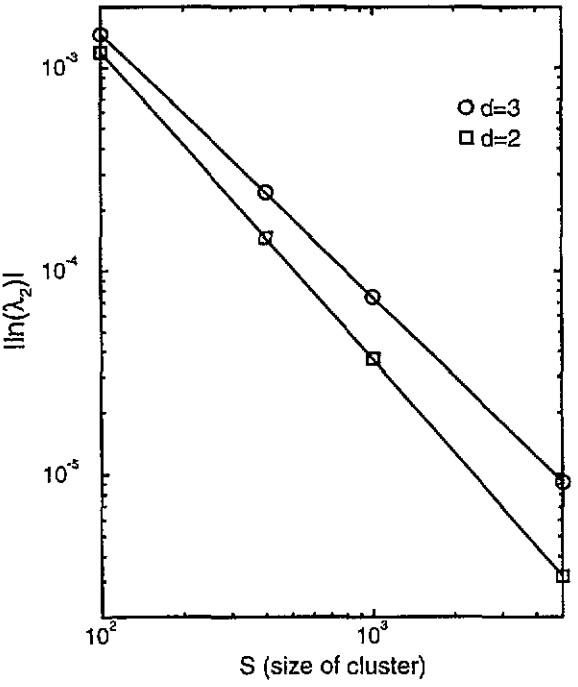

Figure 4. The average of the second largest eigenvalue λ_2 of the transition probability matrix are plotted on logarithmic scales against the cluster size S. The full lines are from least-squares fitting with the slopes of about -1.515 ± 0.002 in 2D and -1.297 ± 0.003 in 3D. The size of the symbols is greater than the statistical fluctuations.

In figure 4 we plot $|\ln\lambda_2|$ against S on logarithmic scales. The straight lines shown are the least-squares fit for which both lines have correlation coefficients greater than 0.999 999. These slopes directly give the ratio d_w/d_f, which allows us to determine the combination $2d_f/d_w$ appearing in (1) to be 1.32 ± 0.01 in two dimensions and 1.54 ± 0.01 in three dimensions. For the sake of comparison with the exact enumeration results, we have combined these results with our estimates for the fractal dimension, d_f, to obtain d_w. These results are summarized in tables 3 and 4.

Table 3. Estimates for d_w, $2d_f/d_w$ and d_s for two dimensions. The Monte Carlo simulation results are taken from Meakin and Stanley [6], and the other results are from this work, where we have taken $d_f = 1.70 \pm 0.02$.

Method	d_w	$2d_f/d_w$	d_s
Monte Carlo [6]	2.56 ± 0.1	1.35 ± 0.1	1.20 ± 0.1
Exact enumeration	2.64 ± 0.05	1.29 ± 0.04	1.20 ± 0.05
Eigenspectrum	2.58 ± 0.04	1.32 ± 0.01	1.16 ± 0.01

Table 4. Estimates for d_w, $2d_f/d_w$ and d_s for three dimensions. The Monte Carlo simulation results are taken from Meakin and Stanley [6], and the other results are from this work, where we have taken $d_f = 2.48 \pm 0.02$.

Method	d_w	$2d_f/d_w$	d_s
Monte Carlo [6]	3.33 ± 0.25	1.44 ± 0.2	1.30 ± 0.1
Exact enumeration	3.19 ± 0.08	1.55 ± 0.06	1.35 ± 0.05
Eigenspectrum	3.21 ± 0.04	1.54 ± 0.01	1.31 ± 0.02

4. Conclusion and discussion

In this work we have calculated the dynamical exponents of diffusion on the DLA in two and three dimensions by the methods of exact enumeration and eigenspectrum analysis. Our results are given in tables 3 and 4 for two and three dimensions, respectively, and are also compared with the earlier work of Meakin and Stanley [6]. Both approaches yield consistent estimates for the exponents d_w, d_s, and the combination d_f/d_w, and unambiguously rules out, in the case of the DLA, the scaling relation (1) proposed by Alexander and Orbach [2]. Thus DLA joins the list of tree-like structures on which this relation is violated.

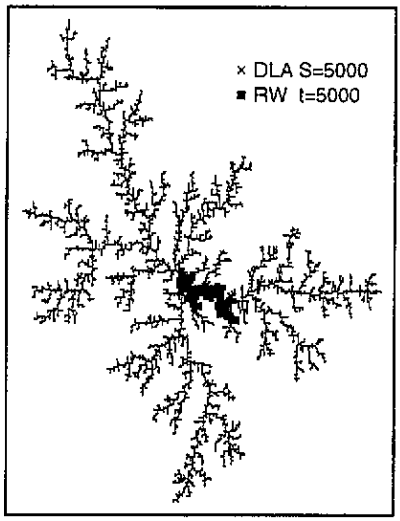

Figure 5. A typical DLA cluster of size 5000 sites is shown together with the trace of a typical random-walk trajectory of 5000 time-steps for the blind-ant rule. The walker starts at the seed site used in generating the DLA.

As in the case of the Eden tree [1, 3], the violation of (1) appears to be due to the trapping of the random walk in a small segment of the DLA, which can be graphically demonstrated by looking at the region visited by the random walk (cf figure 5). It is not simply a matter of how many distinct sites the random walker explores in time t, nor whether the structure

is loopless. We note that, in general, the diffusion on random self-similar fractals will be anomalously slow where (2) holds with $d_w > 2$. On the other hand, we have found that loopless site percolation clusters do obey (1), although the exponents of diffusion differ from normal site percolation clusters [14]. These loopless clusters were made by removing a fraction of the bonds in a prescribed way which eliminates all loops but keeps all the sites in the cluster intact.

There appears to be two necessary ingredients for $d_s = 2d_f/d_w$ to breakdown. The random walker needs to be trapped into local regions of a cluster, as happens for loopless structures, and that these local regions visited by the random walker do not share the same global fractal dimension of the cluster. A future task of great interest would be to develop a systematic theory of the trapping and the anisotropy in diffusion which must be associated with it.

Acknowledgments

DJ would like to thank Professor M Ernst for discussions and Purdue Physics Department for hospitality during his short visits and special thanks to T Statnick for arranging computer time to complete this project. DJ is supported by 'Stichting voor Fundamenteel Onderzoek der Materie (FOM)'. SM and HN appreciate discussions with H Herrmann and N H Fuchs. This work was carried out in part at Purdue and in part at Utrecht.

References

[1] Dhar D and Ramaswamy R 1985 *Phys. Rev. Lett.* **54** 1346–9
[2] Alexander S and Orbach R 1982 *J. Physique Lett.* **43** 625
[3] Nakanishi H and Herrmann H J 1993 *J. Phys. A: Math. Gen.* **26** 4513–19
[4] Witten T A and Sander L M 1983 *Phys. Rev.* B **27** 5686–97
[5] Vicsek T 1989 *Fractal Growth Phenomena* (Singapore: World Scientific)
[6] Meakin P and Stanley H E 1983 *Phys. Rev. Lett.* **51** 1457
[7] Webman I and Grest G S 1985 *Phys. Rev.* B **31** 1689
[8] Jacobs D J and Nakanishi H 1990 *Phys. Rev.* A **41** 706–19
[9] Jacobs D J and Nakanishi H 1993 Physica **197A** 204–22
[10] Fuchs N H and Nakanishi H 1991 *Phys. Rev.* A **43** 1721
[11] Nakanishi H, Mukherjee S and Fuchs N H 1993 *Phys. Rev.* E **47** R1463
[12] Mukherjee S, Nakanishi H and Fuchs N H *Phys. Rev.* E submitted
[13] Saad Y 1980 *Linear Algebra Appl.* **34** 269
[14] Mukherjee S and Jacobs D J 1994 Private communication